7

6

Reprinted from JOURNAL OF ATMOSPHERIC AND OCEANIC TECHNOLOGY, Vol. 6, No. 3, June 1989
American Meteorological Society

Comparison of Simulated Rain Rates from Disdrometer Data Employing Polarimetric Radar Algorithms

N. BALAKRISHNAN AND DUSAN S. ZRNIĆ

JULIUS GOLDHIRSH AND JOHN ROWLAND

Comparison of Simulated Rain Rates from Disdrometer Data Employing Polarimetric Radar Algorithms

N. BALAKRISHNAN* AND DUSAN S. ZRNIĆ

NOAA, Environmental Research Laboratories, National Severe Storms Laboratory, Norman, Oklahoma

JULIUS GOLDHIRSH AND JOHN ROWLAND

The Johns Hopkins University, Applied Physics Laboratory, Laurel, Maryland

(Manuscript received 9 May 1988, in final form 21 October 1988)

ABSTRACT

Disdrometer data collected during three spring days, with moderate to heavy rain in the Norman, Oklahoma region are used with various polarimetric radar algorithms to simulate rain rates. It is assumed that available measurables are 1) reflectivity at horizontal polarization, Z_H, 2) differential reflectivity, Z_{DR} (ratio of horizontal to vertical reflectivity factors in dB), and 3) differential propagation constant, K_{DP}. The accuracies of the simulated rain rates from Z_H, Z_{DR}, and K_{DP} are evaluated and compared. A new algorithm that utilizes both reflectivity factor and differential propagation constant is also examined. In comparing the relative accuracies, the disdrometer-derived rain rates are assumed to be the "truth" measurements.

1. Introduction

Single-parameter radar systems are capable of measuring the radar backscattered power (hence the reflectivity factor Z) and estimating the rain rate R through the use of empirical means. Inherent in these estimators is the assumed form of the drop-size distribution (DSD) and its characterization through a single parameter. Since the DSD is often highly variable, being dependent on the type of precipitation (i.e., convective or stratiform), many empirical rain-rate–radar-reflectivity $R(Z)$ relationships have evolved (Battan 1973; Doviak and Zrnić 1984). The estimation of rain from Z measurements are often plagued by large uncertainties. A radar with linear polarization diversity provides estimates of two parameters, namely, Z_H and Z_V, the reflectivity factors of the hydrometeors for horizontally and vertically polarized illuminations. Seliga and Bringi (1976) demonstrated the use of differential reflectivity Z_{DR} and either the reflectivity factor or K_{DP} (Seliga and Bringi 1978) to estimate two parameters of the DSD. Assuming sufficiently small measurement uncertainties, this technique may lead to more accurate estimates of rain rates (Ulbrich and Atlas 1984).

In addition to reflectivity and differential reflectivity, the differential propagation constant (K_{DP}) has been recently demonstrated to be potentially useful in estimating rainfall rate (Jameson 1985; Mueller 1984; Sachidananda and Zrnić 1986). Because of its relative insensitivity to DSD variations, it has become possible to obtain a more accurate single-parameter estimate of rain rate through an $R(K_{DP})$ empirical relationship (Sachidananda and Zrnić 1987) without calibration worries. This empirical $R(K_{DP})$ relationship, which is based on a Marshall–Palmer distribution, has been found to be useful within acceptable accuracies for simulated gamma DSDs.

The majority of radar algorithms to estimate rain rates are influenced by the variability of DSDs. In order to quantify such effects, one may resort to simulations using artificially contrived DSDs or to disdrometer measurements in natural rain. In the past, disdrometer data have been used to characterize the rain types and to develop theoretical models for the drop-size distribution. In conjunction with a radar and/or raingauge, the disdrometer has been used to validate the rain rate predictions based on $R(Z_H)$ and $R_{ZDR}(Z_H, Z_{DR})$ algorithms. This has also aided in drawing up several useful empirical relationships between the rain rate and the radar observables (Seliga, Aydin and Direskeneli 1986).

But, as pointed out by Chandrasekar and Bringi (1986), caution must be exercised when extrapolating disdrometer measurements to multiparameter radar estimates. Statistical relationships between variables (e.g., Z_H and Z_{DR}) obtained from disdrometer DSDs and radar measurements are different. Z_H and Z_{DR},

* This work was performed while author was a research associate of U.S. National Research Council, Washington, DC, on leave from the Indian Institute of Science, Bangalore, India.

Corresponding author address: Dr. N. Balakrishnan, National Severe Storms Laboratory, 1313 Halley Circle, Norman, OK 73069.

calculated from the disdrometer, are highly correlated and hence, simulated rain-rate errors do not account for these types of statistical uncertainties. We examine the effects of the statistical measurement errors on various rain-rate algorithms, and show that statistical errors due to the Poisson-distributed fluctuations in the particle concentration measured by the disdrometer do not affect our comparisons, if a sufficiently large number of measurements are considered. Simulation with disdrometer data is useful to gauge biases in expected radar measurements, to verify theoretical (or empirical) relationships between derived and measured quantities, to establish relative sensitivities of algorithms to DSD variations, as well as to establish lower bounds on errors.

Although other investigators have examined $R(Z_H)$ and $R_{ZDR}(Z_H, Z_{DR})$ algorithms through disdrometer measurements, no attempt has so far been made to validate the K_{DP}-based rain rate prediction and compare its performance with other techniques, which is an objective of this paper. Our results are based on simulating and analyzing the radar observables from the disdrometer data collected over three rain days in 1986. The disdrometer data are first compared with the rain rate measured by a tipping-bucket raingauge, located nearby (about 5 m), for the purpose of verifying the calibration of the disdrometer. The disdrometer data is subsequently used to compute the relevant dual polarized radar observables such as Z_H, Z_{DR} and K_{DP}. These in turn lead to rainfall rates based on $R(Z_H)$, $R_{ZDR}(Z_H, Z_{DR})$ and $R(K_{DP})$ algorithms. Comparison of these estimates, with the rain rate computed from DSD measured by the disdrometer, has shown that $R(K_{DP})$ is more accurate in its prediction than the other estimators. The statistical measurement errors in the disdrometer estimates and their effect on the comparison of the algorithms are also studied.

Finally, a new method that uses both reflectivity and differential propagation constant is proposed to estimate two parameters of the DSD. The rain-rate estimate based on this technique has been shown to yield marginally improved accuracies compared to the $R(K_{DP})$ algorithm.

2. Simulation method

In the analysis presented here the drop-size distribution $N(D_i)$, as measured by the disdrometer, has been employed to infer Z_H, Z_V, and Z_{DR}. The axis ratio (b/a) was obtained from the data of Pruppacher and Beard (1970). The terminal velocity of the drops v is related to the drop diameter D (in mm) through the empirical relationship (Atlas and Ulbrich 1977):

$$v(D) = 3.778(D)^{0.67} \text{ m s}^{-1}, \quad (1)$$

which produced indistinguishable polarization variables from the ones that are obtained using tabulations by Gunn and Kinzer (1949).

The refractive index of water at 10-cm wavelength and 0°C has been taken as (Ray 1972)

$$m = 9.035 + j1.394. \quad (2)$$

The axis ratio and the refractive index were used to compute the radar cross sections σ_H and σ_V (Seliga and Bringi 1976) for horizontally and vertically polarized waves. The differential propagation constant for each drop size has been computed based on the techniques of Oguchi 1983. Using these parameters, the radar observables have been computed for each of the disdrometer distributions. The disdrometer-derived rain rate has been calculated using the relationship

$$R_{\text{dis}} = 0.6\pi \times 10^{-3} \sum_{i=1}^{M} v(D_i) D_i^3 N(D_i) \Delta D_i \text{ mm h}^{-1}, \quad (3)$$

where M is the number of categories of drop diameters measured by the disdrometer, $N(D_i)$ is the number of drops in m^{-3} mm^{-1} between diameters $D_i - \Delta D_i/2$ and $D_i + \Delta D_i/2$ and terminal velocity v is in m s^{-1}. In the case of the disdrometer used, D_i's are spaced 0.1 mm apart between 0.2 mm and 5.8 mm, therefore, M is equal to 57.

3. Rainfall rate estimation from dual polarization radar algorithms

Seliga and Bringi (1976) proposed a technique to estimate the parameters N_0 and D_0 that describe an exponential raindrop size distribution

$$N(D) = N_0 \exp(-3.67 D/D_0) \quad 0 \leq D \leq D_{\max}. \quad (4a)$$

This form of distribution is a special case of the more general gamma drop-size distribution (DSD) defined as

$$N(D) = N_0 D^{\mu} \exp(-\lambda D) \quad 0 \leq D \leq D_{\max}, \quad (4b)$$

where $N_0(\text{m}^{-3}\ \text{mm}^{-1-\mu})$, μ and $\lambda(\text{mm}^{-1})$ are the parameters of the DSD. The technique requires an assumption for the maximum drop diameter $D_{\max}$. Previously employed values are in the range of 6 to 8 mm, and we have used 7 mm in one set of calculations. Because our disdrometer data did not contain sizes larger than 5 mm, we also used this more realistic value in various algorithms. Since Z_{DR} is independent of N_0, it can be used to estimate directly D_0, the median volume diameter when $D_{\max} = \infty$; D_0 in conjunction with either the reflectivity factor Z_H or the differential propagation constant K_{DP}, yields N_0. Once N_0 and D_0 are known, it is straightforward to obtain the rain rate. This technique uses tabulations (Seliga and Bringi 1976) depicting the variations of Z_{DR} and either Z_H/N_0 or K_{DP}/N_0 with D_0. The rain rate estimated from this algorithm is denoted as $R_{ZDR}(Z_H, Z_{DR})$ in this paper. Goldhirsh et al. (1987) have been successful in comparing lower rain rates using such a technique on data from a multiple-polarization radar and rain gauge.

Subsequently, several empirical relationships have been developed to estimate directly the rain rate from Z_H and Z_{DR}. Notable amongst them are (Ulbrich and Atlas 1984; Seliga et al. 1986):

$$R_{\text{exp}}(Z_H, Z_{DR}) = 1.93 \times 10^{-3} Z_{DR}^{-1.5}(10^{0.1Z_H}) \quad (5a)$$

for exponential DSD, and

$$R_{\text{gam}}(Z_H, Z_{DR}) = 1.70 \times 10^{-3} Z_{DR}^{-1.5}(10^{0.1Z_H}) \quad (5b)$$

for gamma DSD with $\mu = 2$, where the rainfall rates are in mm h^{-1}, Z_{DR} in dB, Z_H in dBZ, and the maximum drop diameter is about 8 mm.

Both empirical relationships are based on the assumption that $\lambda D_{\max}$ is large, so that the integrals involving DSD and its moments can be taken to extend to infinity and hence are independent of $D_{\max}$. In the case of Z_{DR}, Ulbrich and Atlas (1984) show that the Z_{DR}–D_0 relationship is independent of $D_{\max}$ variations when $D_{\max}/D_0 > 2.5$ for Eq. (5a) and ≥ 2.0 for Eq. (5b).

Because the differential propagation constant has been found to be relatively insensitive to DSD variations, Sachidananda and Zrnić (1987) proposed the following direct empirical relationship between K_{DP} and R:

$$R(K_{DP}) = 20.35(K_{DP})^{0.866}. \quad (6)$$

This relationship is based on an assumed Marshall–Palmer distribution, wherein N_0 is taken as constant (8000 m^{-3} mm^{-1}), $D_{\max}$ is large and hence for all practical purposes, infinite, and K_{DP} is in deg km^{-1}.

Seliga and Bringi (1978) proposed use of Z_{DR} and K_{DP} to obtain two parameters of the DSD, in a manner similar to that from Z_{DR} and Z_H. Of these dual polarization measurables, Z_{DR} and Z_H are affected by both anisotropic hydrometeors like rain, as well as isotropic hydrometeors such as tumbling or spherical hail. K_{DP} is not affected by isotropic scatterers; but, the parameters of the drops distribution in the mixture cannot be obtained from K_{DP} alone. The parameters N_0 and D_0 are required for studies of the evolution of the DSD and they should provide a better estimate of rain water in the mixture. This has motivated us to examine the descriptor:

$$Q = \frac{Z_H - Z_V}{K_{DP}}, \quad (7)$$

where Z_H and Z_V are in mm^6 m^{-3} and K_{DP} is in deg km^{-1}. Statistically, isotropic scatterers contribute equally to Z_H and Z_V but K_{DP} is independent of such scatterers. Hence, Q depends only on the anisotropy of the hydrometeors (e.g., rain). It must not be construed that Q will only be useful for mixed-phase hydrometeors; it may be applied to pure rain as well and this is examined in the following paragraphs.

For an exponential or gamma type of DSD such as given by (4a) or (4b), Q is independent of N_0. Figure 1 shows the variations of Q with D_0 for a $D_{\max}$ of 7 mm. The measured value of Q could be used to obtain D_0, whereas N_0 could be obtained from K_{DP} and D_0.

For equal-size scatterers, it can be shown in the Rayleigh limit that

$$Q = C\frac{|S_{HH}|^2 - |S_{VV}|^2}{R_e(S_{HH} - S_{VV})} \approx C|S_{HH} + S_{VV}|$$

$$\approx CR_e(S_{HH} + S_{VV}), \quad (8)$$

where S_{HH} and S_{VV} are the diagonal terms of the scattering matrix and C is a proportionality constant. Other assumptions used in deriving (8) are: 1) phase shifts upon scattering are small so that imaginary contributions to the magnitudes in the numerator are negligible, and 2) attenuation is negligible so that S_{HH} and S_{VV} are real, and 3) the precipitation is constant in the propagation path over which K_{DP} is measured.

The magnitude and hence the real part of $S_{HH} + S_{VV}$ are independent of canting angles (McCormick and Henry 1975). Jameson (1986) has obtained the following relationship:

$$R_e(S_{HH} + S_{VV}) = (8.760 \times 10^{-2})D^{3.034}. \quad (9)$$

Because (9) is almost proportional to D^3, the liquid water content is linearly related to $S_{HH} + S_{VV}$ regardless of the DSD; it is also independent of canting angle distributions. It should be pointed out that for real distributions Q would not be independent of DSD variations. It has the advantage that it could be estimated readily from dual-polarized radar data, however. This is particularly attractive since a direct measurement of $|S_{HH} + S_{VV}|$ is difficult in practice.

Using Eq. (9) and the fact that K_{DP} [and hence $(S_{HH} - S_{VV})$] is proportional to $D^{4.24}$ (Sachidananda and Zrnić 1986), it can be shown that for a gamma DSD [Eq. (4b)],

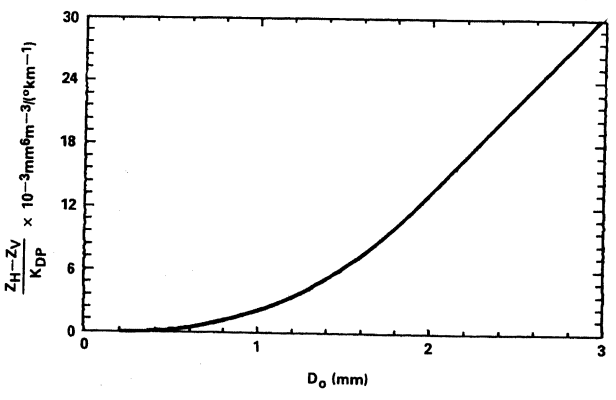

FIG. 1. Variations of $(Z_H - Z_V)/K_{DP}$ with D_0. The exponential DSD [Eq. (4a)] is used.

$$Q = \frac{c\int_0^{D_{\max}} (S_{HH} + S_{VV}) N_0 D^{(4.24+\mu)} e^{-\lambda D} dD}{\int_0^{d_{\max}} N_0 D^{(4.24+\mu)} e^{-\lambda D} dD}. \quad (10)$$

The denominator represents the total number of particles in the DSD weighted by $D^{4.24}$. It is then apparent that Q is indeed the average value of $(S_{HH} + S_{VV})$ over the DSD that is modified by the weight $(S_{HH} - S_{VV})$. For $\lambda D_{\max} \to \infty$, Q reduces to

$$Q = c \times \frac{\Gamma(8.24 + \mu)}{\Gamma(5.24 + \mu)} \times \frac{D_0^3}{(3.67 + \mu)^3}, \quad (11)$$

where c is a constant, $\Gamma(x)$ is the gamma function, and D_0 is the median volume diameter.

The fact that Q, expressed in terms of Z_H, Z_V and K_{DP}, is proportional to $|S_{HH} + S_{VV}|$ and that it can be measured and used to estimate anisotropic precipitation has prompted us to explore its applicability for realistic drop-size distributions. The rainfall rate derived from Q, $R_Q(Z_H, Z_V, K_{DP})$, is depicted in Fig. 2 for a few gamma drop-size distributions. Note that rain rates in the range of 30–50 mm h^{-1} are minimally sensitive to variations in μ.

4. Disdrometer and raingauge measurements

An impact-type disdrometer developed by Rowland, (1976), has been used for measuring drop-size distributions. Such a disdrometer has been successfully employed in establishing empirical relations between radar attenuation coefficient and reflectivity ($k - Z$) for estimating slant path attenuation above 10 GHz using S-band radar measurements (Goldhirsh 1979, 1980), and also to study rain cell sizes of various rain rates (Goldhirsh and Musiani 1986). This disdrometer is capable of measuring drop sizes from 0.2 mm through 5.8 mm with a resolution of 0.1 mm.

The disdrometer diameter is two inches. Each distribution is obtained after the disdrometer has sampled 2000 drops. Hence the sampling time and the sampling

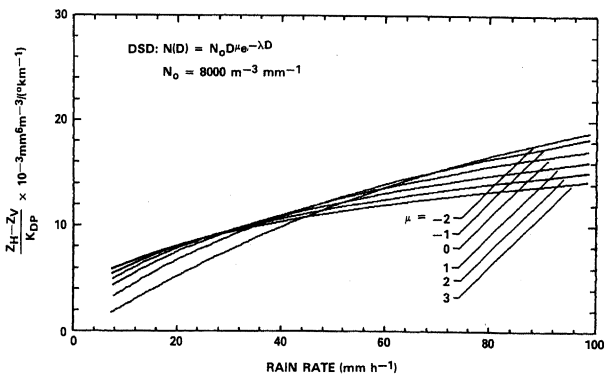

FIG. 2. Plots of $(Z_H - Z_V)/K_{DP}$ with rain rate for various gamma raindrop-size distributions.

TABLE 1. Overview of the disdrometer data.

Day	Time (CST) From (h–min–s)	Time (CST) To (h–min–s)	Total number of distributions	Average rain rate (mm h^{-1})	Max. rain rate (mm h^{-1})
134	16–51–02	18–54–05	308	26.76	79.09
136	21–35–39	22–52–12	136	9.52	16.73
155	14–52–18	16–18–58	218	12.62	39.24

volume are dependent on the rainfall rate. The sampling time is larger for lower rain rates. It is typically 25 s when the rain rate is 20 mm h^{-1}. The sampling volume depends also on the fall velocity of the drops and is equal to $A \times v(D) \times t$ where A is the area of the disdrometer in m^2, $v(D)$ is the drop velocity in m s^{-1}, and t is the sampling time in s.

The database examined consisted of a total of 662 distributions obtained at the National Severe Storms Laboratory in Norman, Oklahoma, during three rain days in 1986; namely, days 134 (14 May 1986), 136 (16 May 1986) and 155 (4 June 1986). A tipping-bucket raingauge located nearby was also used to collect rain rate information and to verify the disdrometer calibration. Table 1 gives a broad overview of the dataset analyzed.

Samples of the measured distributions are given in Fig. 3a for rain rates between 40 mm h^{-1} and 50 mm h^{-1} and in Fig. 3b for rain rates less than 10 mm h^{-1}. At rain rates between 40 and 50 mm h^{-1}, it can be seen that there are no drops recorded beyond 4 mm, while for rain rates less than 10 mm h^{-1}, the maximum drop size is 2.3 mm. In the entire data set of 662 distributions, the maximum drop size recorded with the disdrometer was 5.2 mm, even though the disdrometer was able to measure up to 5.8 mm.

The rain rate R_{dis} given by (3) is compared with that measured by the raingauge, R_g in Figs. 4a and 4b. These curves are derived using a two-minute average of both R_{dis} and R_g for 14 May 1986 and 4 June 1986, respectively. The averaging was performed to coalesce the integration times of the disdrometer and the raingauge, and hence it reduces the standard errors in rain rates measured by both these devices. It can be seen from the figures that the two rain rates show generally good comparison. There are deviations, however, between the rain gauge and the disdrometer rain rates at higher rainfall rates, most likely because the sampling volume of the disdrometer is very limited, especially for large drops. This does not influence our simulations whatsoever.

5. Comparisons of different algorithms for rainfall estimation

The rainfall rate estimates from the algorithms $R(Z_H)$, $R_{ZDR}(Z_H, Z_{DR})$, $R_{\exp}(Z_H, Z_{DR})$, $R_{\text{gam}}(Z_H, Z_{DR})$, $R(K_{DP})$ and $R_Q(Z_H, Z_V, K_{DP})$ are computed for

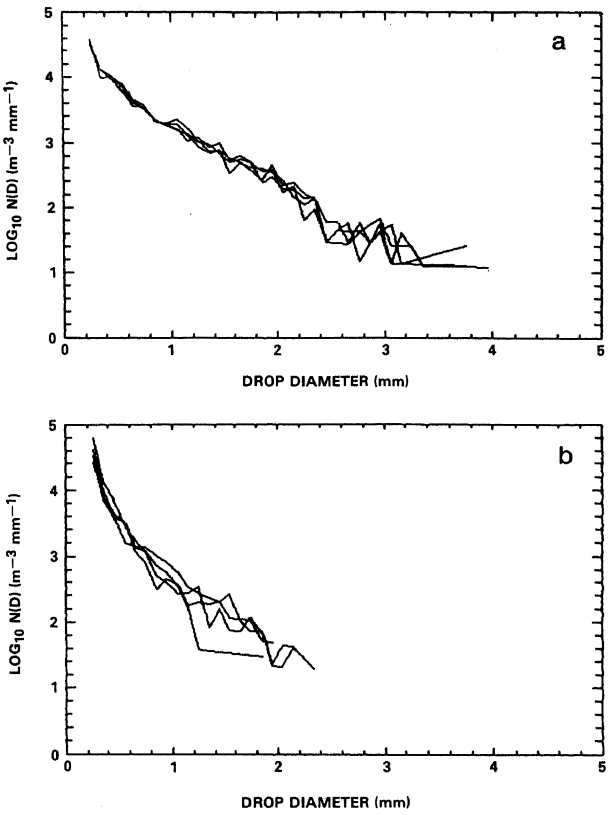

FIG. 3. (a) Samples of four raindrop-size distributions measured by the disdrometer for typical rain rates between 40 mm h^{-1} and 50 mm h^{-1}. (b) Same as (a) but for typical rain rates below 10 mm h^{-1}.

all 652 distributions measured by the disdrometer. They are compared with R_{dis}, obtained from the disdrometer, and the results are presented in the following paragraphs. In our analysis the $R - Z$ relationship has been obtained by the least-squares-fitting R_{dis} to aZ^b. The Marshall–Palmer relationship $Z = 200R^{1.6}$ (Battan 1973) and $Z = 367R^{1.42}$ (Ulbrich and Atlas 1984) have also been compared.

Figure 5 shows the scatter plot of Z_H and Z_{DR} for all the distributions considered. From the figure it can be seen that there is a clear boundary defining a preferential set of Z_H, Z_{DR} values for rain. This fact was originally observed in radar data by Leitao and Watson (1984) and deduced from disdrometers by Aydin et al. (1986). The latter used departures from this boundary for pure rain to derive a new hail signal. Our data are, by a good margin, on the correct side of the boundary.

The scatter plot of K_{DP} and Z_H is shown in Fig. 6. The tight clustering of points in this figure suggests that Z_H versus K_{DP} could be used as a better discriminator of rain and nonrain hydrometeors.

Results of the comparison of various rainfall estimates with the rain rate R_{dis} obtained from the disdrometer data are presented in Table 2. In calculations leading to these results, values of D_{max} suggested by investigators that developed the algorithm were used; these were 7 mm and greater. The table includes the maximum (Max. %) and average absolute values (AAD %) of the deviation $|R_e - R_{dis}|/R_{dis} \times 100\%$, where R_e is the rain rate estimated from the radar observables. The rms values of the deviation are given only for the combined dataset because they are very similar to AAD values on individual days.

Note that for a fixed $R - Z_H$ relationship the AAD is high in the range of 32%–52%, which agrees in general with the findings of Ulbrich and Atlas (1984). However, if the $R - Z_H$ relationship is adjusted using disdrometer measurements so that the squared deviation is minimized, the AAD is reduced to a range of 12%–23%. The rain rates predicted using Z_H and Z_{DR} for the combined set give AAD and rms deviations in the neighborhood of 19% and 23%, respectively. Ulbrich and Atlas (1984) found an AAD of 27% in $R(Z_H, Z_{DR})$. The errors in $R(K_{DP})$ and R_Q are markedly lower at 12.5% and 7.4% for AAD, respectively. There are two aspects that are worth noting. First, the $R(K_{DP})$ performs relatively better than the algorithms based on Z_H and Z_{DR}. Second, when a second parameter of DSD

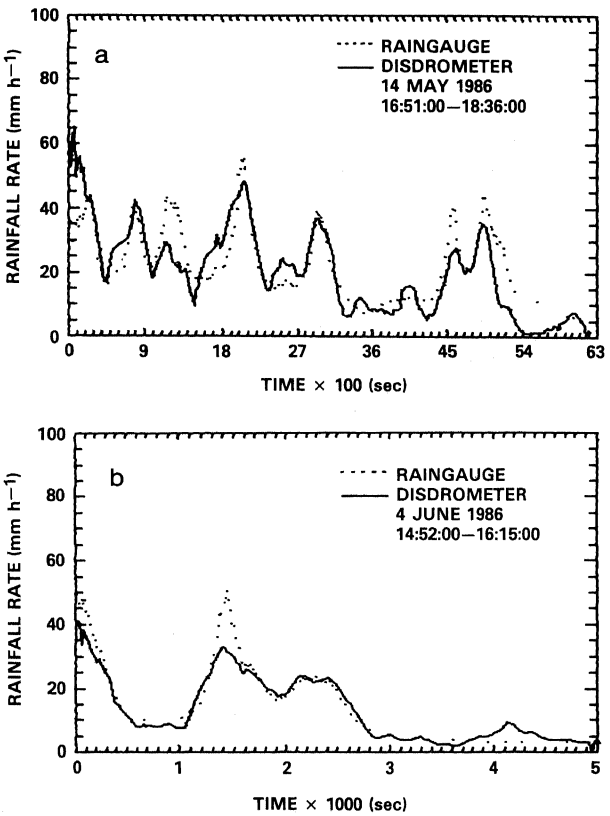

FIG. 4. (a) Rainfall rates measured by rain gauge and disdrometer on 14 May 1986 (two-minute averages). (b) Same as in (a) but on 4 June 1986.

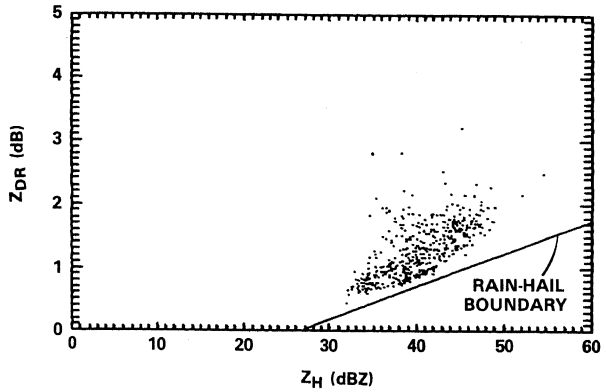

FIG. 5. Scattergram of Z_H and Z_{DR} simulated from the distributions measured by the disdrometer (three days).

is estimated through the use of Z_H and Z_{DR}, the AAD is, at best, reduced to 17.5% compared to $M - P\,R(Z_H)$ relationship, which gave a combined AAD of 35.6%. Improvements of such magnitude are not seen between $R(K_{DP})$ and $R_Q(Z_H, Z_V, K_{DP})$, however. This is consistent with the fact that $R(K_{DP})$ is relatively independent of DSD variations as previously noted. The scatter plots of the deviations for the entire data set are given in Fig. 7 to Fig. 10, for $R(Z_H)$, $R_{ZDR}(Z_H, Z_{DR})$, $R(K_{DP})$ and $R_Q(Z_H, Z_V, K_{DP})$, respectively. The scatter plot of $R(Z_H)$ is based on $Z = 367R^{1.42}$ given by Ulbrich and Atlas (1984).

The performance of $R(Z_H, Z_{DR})$ algorithm warrants further consideration. For the data on 4 June 1986, $R(Z_H, Z_{DR})$ gives larger AAD than the best fit $R(Z_H)$, though much less than fixed $R(Z_H)$ estimators. The scatter plot presented in Fig. 8a for $R(Z_H, Z_{DR})$ shows that there is a systematic offset of the estimate above the actual rain rate calculated from the disdrometer distributions. This observation is similar to that reported by Atlas and Ulbrich (1977) and Ulbrich and Atlas (1984). They attributed these effects, due to the inadequacy of the exponential distribution [Eq. (4a)], to represent the shape variations in the measured DSD. Using the theoretical $Z_{DR} - D_0$ relationship for a gamma distribution [Eq. (4b)] with $\mu = 2$ and large D_{max}/D_0, Ulbrich and Atlas (1984) showed that AAD for their dataset reduced (from 27%) to 14%. This is represented by $R_{gam}(Z_H, Z_{DR})$ given by Eq. (5b). For our dataset, however, we find that $R_{gam}(Z_H, Z_{DR})$ with $\mu = 2$, (Table 2) gives no such improvement. In fact, the AAD for the gamma distribution with $\mu = 2$ is larger (21.2%) than that of $R_{exp}(Z_H, Z_{DR})$ (19.1%). Ulbrich and Atlas (1984) observe that the better performance of $R_{gam}(Z_H, Z_{DR})$, in their case, is due and consistent with their observation that "the particular dataset of drop size spectra used in their work shows a tendency toward downward concavity and is consequently better described by a DSD like Eq. (4b) with $\mu > 0$" (Ulbrich and Atlas 1984).

In contrast, the DSD presented in Figs. 3a and 3b are almost linear, particularly in the medium drop-size regions. All the DSD's measured are similar to those in Figs. 3a and 3b. They exhibit a small tendency toward upward concavity and a reduced maximum drop diameter. The latter is more pronounced. The shape parameter $S(Z\sigma)$, where Z is the reflectivity factor and σ is the optical extinction, defined by Joss and Gori (1978), is found to be >1 for the majority of the distributions. This is in conformity with the small upward concavity seen in Figs. 3a and 3b. The upward concavity can be satisfied by a gamma distribution with $\mu < 0$. Such a distribution, however, is characterized by broader drop-size spectrum and larger D_{max} than the exponential distribution. Such a distribution, furthermore, cannot account for the positive offset observed in Fig. 8a.

Analysis of all 662 distributions showed that for nearly 50% of the distributions D_{max}/D_0 was less than 2.5. It is probable that inadequate sampling by the disdrometer contributed to the failure to detect larger drops. Alternately, physical mechanisms may be responsible in restricting the maximum drop diameter. Whatever the actual reason, such effects explain the offset observed in Fig. 8a for the dataset used in this study.

The effects of DSD truncation due either to physical or instrument dependent causes, are studied in detail by Ulbrich (1985) and Ulbrich and Atlas (1984). They establish the limits on D_{max}/D_0 beyond which the truncation effects are negligible. Ulbrich (1985) furthermore shows that a precipitation parameter deduced from a pair of remote measurables like Z_H and Z_{DR}, depends on DSD shape and DSD truncation through a multiplicative factor only. These prompted us to explore the use of a realistic D_{max} based on the observed DSD, to improve the performance of $R(Z_H, Z_{DR})$.

It should be pointed out that $R_{ZDR}(Z_H, Z_{DR})$ has been obtained using the $Z_{DR}(D_0)$ and $Z_H(N_0, D_0)$ curves computed with a D_{max} of 7 mm, whereas for

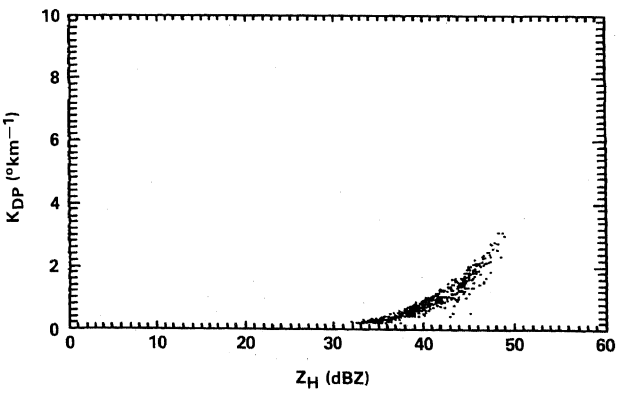

FIG. 6. Scattergram of Z_H and K_{DP} simulated from the distributions measured by the disdrometer (three days).

TABLE 2. Comparison of algorithms for rainfall estimation ($D_{max} \gtrsim 7$ mm).

No.	Rainfall estimator	14 May 1986 Max (%)	14 May 1986 AAD (%)	16 May 1986 Max (%)	16 May 1986 AAD (%)	4 June 1986 Max (%)	4 June 1986 AAD (%)	Combined Max (%)	Combined AAD (%)	Combined Rms (%)
1	$R(Z_H)\ M-P\ Z=200\ R^{1.6}$	−237.8	31.5	−204.7	28.3	56.0	44.4	−237.8	35.6	39.7
2	$R(Z_H)\ Z=367\ R^{1.42}$	−226.0	35.0	−184.1	32.4	63.0	51.9	−226.0	42.1	45.0
3	$R\ (Z_H)$ (best fit)	−319.4	21.8	−279.8	22.9	−106.5	12.1	−351.0	19.1	33.7
4	$R_{exp}\ (Z_H, Z_{DR})$	79.9	17.4	85.0	21.0	69.1	14.8	85.0	17.5	21.8
5	$R_{gam}\ (Z_H, Z_{DR})$	82.3	21.4	83.8	20.9	76.8	20.0	83.8	21.2	26.3
6	$R_{ZDR}\ (Z_H, Z_{DR})$	−42.1	17.2	−32.4	13.8	−39.7	24.0	−42.1	19.0	23.6
7	$R(K_{DP})$	−75.3	10.4	−78.7	9.4	24.8	16.9	−78.7	12.5	14.6
8	$R_Q\ (Z_H, Z_V, K_{DP})$	−29.0	6.2	20.8	3.8	−23.4	10.9	−29.0	7.4	9.1

the $R(K_{DP})$ relationship D_{max} was 10 mm (practically infinite). The effect of D_{max} on K_{DP} and Z_H would be pronounced at higher rain rates (e.g., $R > 40$ mm h^{-1}). When the measured distribution has a smaller D_{max}, the computed K_{DP} would be less, and the $R(K_{DP})$ algorithm [Eq. (6)] would consistently underestimate the rain rate. This is also in conformity with what is seen in Fig. 9. The change in K_{DP} for a D_{max} variation from 7 mm to 5 mm would be of the order of 5%, producing a 4.3% change in rain rate (Sachidananda and Zrnić 1986). Since the offsets in $R(K_{DP})$ (Fig. 9) and R_Q (Fig. 10) are small (Figs. 11 and 12), no adjustments are necessary when employing the corresponding algorithms.

These considerations point out that a proper choice of D_{max} could reduce the systematic errors in $R_{ZDR}(Z_H, Z_{DR})$ and if desired, in $R(K_{DP})$. The $Z_{DR}(D_0)$ and $Z_H(N_0, D_0)$ values were modified using the values obtained for truncated exponential distributions with D_{max} of 5 mm. The scatter plot of $R_{ZDR}(Z_H, Z_{DR})$ and R_{dis} for the reduced D_{max} of 5 mm is shown in Fig. 8b. Note that the offset is substantially reduced. The $R(K_{DP})$ algorithm (Fig. 11) is also modified with the above choice of D_{max} to

$$R(K_{DP}) = 22.72(K_{DP})^{0.867}. \qquad (12)$$

Employing the more realistic D_{max} of 5 mm, it was observed (Table 3) for the combined dataset that AAD for $R_{ZDR}(Z_H, Z_{DR})$ reduced to 10.3% and the rms deviation to 14.5%. The corresponding performance measures for R_Q are 7.4% and 8.4%, respectively. The $R(K_{DP})$ estimates are nearly as good as the ones obtained from R_Q (Fig. 12) showing the AAD and rms deviations to be 7.9% and 10.4%, respectively.

6. Measurement error and its contribution to AAD

The AAD's given in Tables 2 and 3 are comprised of two quantities. They are (i) the contribution due to

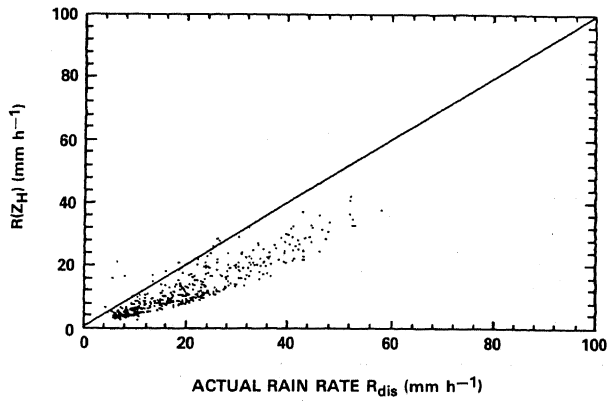

FIG. 7. Comparison of rainfall rates calculated from simulated measurements of Z_H with the actual rate R_{dis} (three days). The $R - Z_H$ relationship $Z = 367R^{1.42}$ is used.

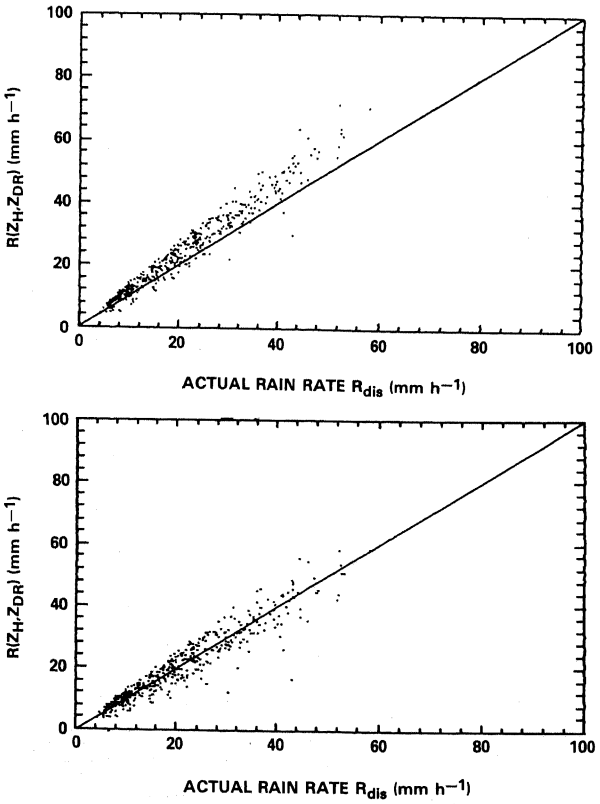

FIG. 8. (a) Comparison of rainfall rates estimated from simulated measurements of Z_H and Z_{DR} with the actual rain rates R_{dis} (D_{max} = 7 mm; three days). (b) Same as in (a) but D_{max} = 5 mm.

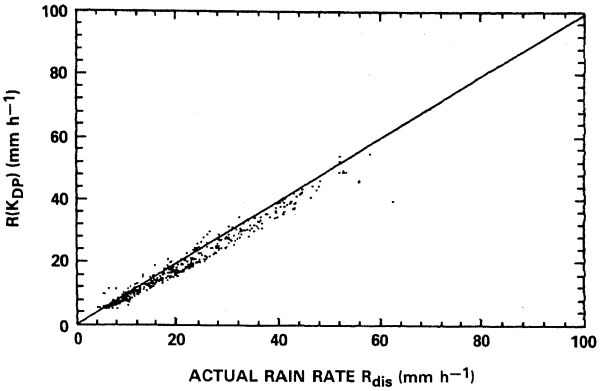

FIG. 9. Comparison of rainfall rates estimated from simulated measurements of K_{DP} with the actual rain rates R_{dis} (D_{max} = 7 mm).

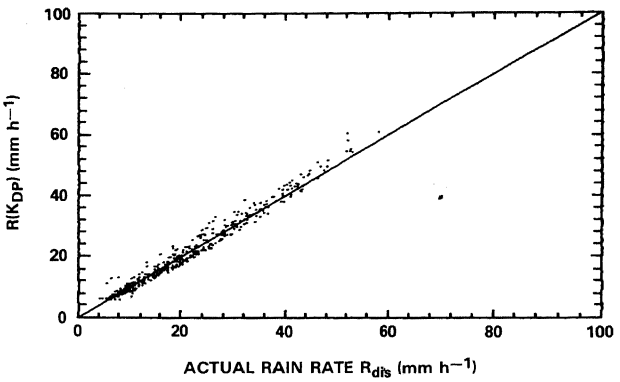

FIG. 11. Same as Fig. 9 (D_{max} = 5 mm).

natural DSD variations (σ_{DSD}/R) and (ii) the contribution due to statistical measurement error in the disdrometer (σ_s/R). It is difficult to separate these contributions from one another. In order to ensure that the comparison of various rain rate algorithms truly reflect their sensitivity to natural DSD variations, however, it is necessary that the dataset used is such that σ_s/R is relatively small for all the algorithms. σ_s/R depends on the sampling volume of the disdrometer, rain rate, number of DSDs averaged in computing the AAD and also the algorithm itself. In this section, it is shown that for the combined dataset used in the present study (Tables 2 and 3), σ_s/R is negligible in the case of $R(K_{DP})$ and $R_Q(Z_H, Z_V, K_{DP})$ and is approximately 2% in the case of $R(Z_H)$ and $R(Z_H, Z_{DR})$.

The statistical measurement errors are due to Poisson-distributed fluctuations of the number of particles sampled by the disdrometer (Gertzman and Atlas 1977). The results in this section assume that the DSD is exponential [Eq. (4a)] with $D_{max} \rightarrow \infty$. The disdrometer specifications (2-in diameter and 25 s sampling time) are taken to match closely those of the actual disdrometer used. The fractional standard deviation (FSD) is used as a measure of the statistical errors. The FSD of a variable x is defined as

$$\mathrm{FSD}(x) = \frac{\sigma_x}{\langle x \rangle}, \tag{13a}$$

and FSD in dB as

$$\sigma_{dB}(x) = 10 \log\left(1 + \frac{\sigma_x}{\langle x \rangle}\right), \tag{13b}$$

where σ_x is the standard deviation of x and $\langle\ \rangle$ represents the expected value. The FSD of a single parameter like R or Z estimated from disdrometer measurement is well studied in Joss and Waldvogel (1969) and Gertzman and Atlas (1977) who used the exponential DSD. Wong and Chidambaram (1985) considered the statistical errors incorporating the gamma DSD. Chandrasekar and Bringi (1986, 1988) showed that the statistical errors in disdrometer derived Z and R are correlated. In this section, we extend these formulations to compute the statistical errors in various rain rate algorithms and their contribution (σ_s/R) to the AADs presented in Tables 2 and 3.

The general form of the rain-rate algorithm is taken as

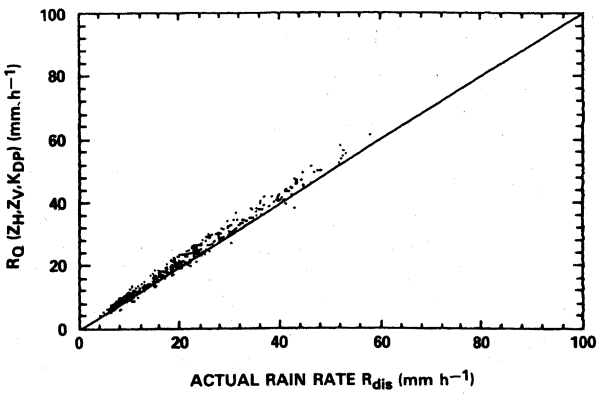

FIG. 10. Comparison of rainfall rates estimated from simulated measurements of $(Z_H - Z_V)/K_{DP}$ and K_{DP} with the actual rain rates R_{dis} (D_{max} = 7 mm).

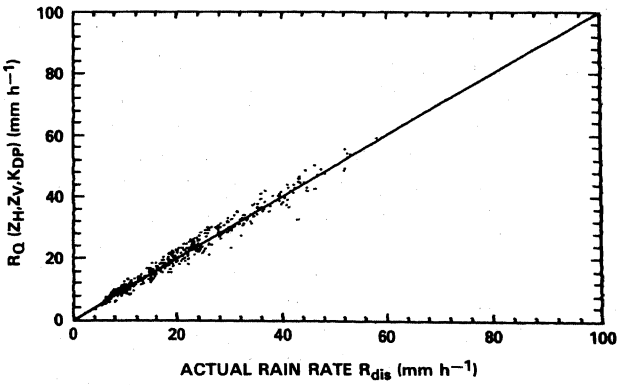

FIG. 12. Same as Fig. 10 (D_{max} = 5 mm).

TABLE 3. Comparison of rainfall estimation with D_{max} = 5 mm.

No.	Rainfall estimator	14 May 1986 AAD (%)	16 May 1986 AAD (%)	4 June 1986 AAD (%)	Combined AAD (%)	Combined Rms (%)
1	$R_{ZDR}(Z_H, Z_{DR})$	11.8	8.3	9.0	10.3	14.5
2	$R(K_{DP})$	6.4	10.6	8.1	7.9	10.4
3	$R_Q(Z_H, Z_V, K_{DP})$	6.3	4.2	10.6	7.4	8.4

$$R_e = aP_1{}^b(10 \log P_2)^c, \tag{14}$$

where a is the coefficient, and b and c are the exponents in the empirical relationship. P_1 and P_2 are the polarimetric estimates obtained from the disdrometer measured DSD. Equation (14) reduces to single parameter algorithms like $R(K_{DP})$ and $R(Z_H)$ when $c = 0$. For $R(Z_H, Z_{DR})$, it is seen from Eqs. (5a) and (5b) that $b = 1$ and $c = -1.5$ when P_1 is Z_H in mm^6 m^{-3} and P_2 is Z_{DR} expressed as the ratio Z_H/Z_V. The absolute deviation is then written as

$$AD = \frac{|\hat{R} - a(\hat{P}_1)^b(10 \log\hat{P}_2)^c|}{\hat{R}}, \tag{15}$$

where $\hat{}$ represents direct or simulated estimate from the disdrometer. Using perturbation analysis, it can be shown that the normalized contributions in AD due to statistical measurement errors alone [i.e. $E(\hat{R})$ equals (14)] is

$$\frac{\sigma_s^2}{\hat{R}^2} = \frac{\text{var}\hat{R}}{\hat{R}^2} + b^2\frac{\text{var}\hat{P}_1}{\hat{P}_1^2} + c^2\frac{\text{var}\hat{P}_2}{\hat{P}_2^2(\ln\hat{P}_2)^2} + b \times c \times \frac{\text{cov}(\hat{P}_2, \hat{P}_1)}{\hat{P}_1\hat{P}_2(\ln\hat{P}_2)} - b\frac{\text{cov}(\hat{R}, \hat{P}_1)}{\hat{R}\hat{P}_1} - c\frac{\text{cov}(\hat{R}, \hat{P}_2)}{\hat{R}(\hat{P}_2 \ln\hat{P}_2)}. \tag{16}$$

It is apparent from Eq. (16) that if estimates of $\hat{R}$, $\hat{P}_1$, and $\hat{P}_2$ are obtained from independent measurements using individual disdrometers sampling the same rain medium, the covariance terms would be zero, and hence $\sigma_s/\hat{R}$ would be larger.

The disdrometer estimates of $\hat{R}$, $\hat{Z}_H$, $\hat{K}_{DP}$ of a single particle of diameter D can be expressed as a power of D. This facilitates the use of simple expressions involving gamma function to calculate the variance terms (Gertzman and Atlas 1977) and the covariance terms (Chandrasekar and Bringi 1986) in Eq. (16). Numerical integration over the exponential DSD is used to obtain the variance of Z_{DR} and its covariance with R and Z_H (Chandrasekar and Bringi 1988).

The FSDs of R, K_{DP}, Z_H and Z_{DR} derived from our disdrometer at 18.56 mm h^{-1} rain rate (the average rainfall of our dataset), are found to be 0.22, 0.32, 0.98 and 0.84, respectively. The FSD, in general, decreases with increasing rain rate (Gertzman and Atlas 1977). From Eq. (13b), it is seen that $\sigma_{DB}(Z_H)$ is 2.97 dB and $\sigma_{dB}(Z_{DR})$ is 2.65 dB. These values are larger than $\sigma_{dB}(Z_H)$ of 1 dB $\sigma_{dB}(Z_{DR})$ of 0.1 dB, and that are theoretically possible for a single measurement (256 samples) from a typical 10-cm radar (Sachidananda and Zrnić 1986). However, the effect of larger statistical errors on the rain-rate algorithm given by Eq. (14) is offset to an extent by the correlations among the disdrometer estimates. For the disdrometer, the statistical error in R at 18.56 mm h^{-1} is found to have correlation of 0.76, 0.98 and 0.33 with that of Z_H, K_{DP} and Z_{DR}. The correlation between the statistical errors in Z_H and Z_{DR} from the disdrometer is found to be 0.89, while it is nearly zero when Z_H and Z_{DR} are obtained from a radar.

In the case of K_{DP}, the disdrometer estimate has smaller FSD (0.32) than is possible with a typical radar ($\approx$1 at 18.56 mm h^{-1}). Further, in a disdrometer, there is a high correlation between the statistical errors in R and K_{DP}. Hence, σ_s/R is smaller for $R(K_{DP})$ obtained from a disdrometer. This is also true of $R_Q(Z_H, Z_V, K_{DP})$.

The statistical errors in radar estimates of Q can be shown to be

$$\frac{\text{var}(Q)}{Q^2} = \frac{\text{var}(Z_H - Z_V)}{(Z_H - Z_V)^2} + \frac{\text{var}(K_{DP})}{K_{DP}^2}, \tag{17}$$

where it is assumed that the radar estimates of $(Z_H - Z_V)$ and K_{DP} are uncorrelated. It is easy to see that the dominant contribution to var(Q) is from the var(K_{DP}). This is because var($Z_H - Z_V$) is very small in a radar. Hence the performance of $R_Q(Z_H, Z_V, K_{DP})$ estimated from a radar, would be poor at low rain rates where the fractional error of K_{DP} is large. In brief, we see that at 18.56 mm h^{-1} rain rate, the statistical errors of radar-derived and disdrometer-simulated rain rates are comparable in the case of $R(Z_H)$ and $R(Z_H, Z_{DR})$ algorithms. The statistical error in disdrometer is less than that of radar measured $R(K_{DP})$ and $R_Q(Z_H, Z_V, K_{DP})$.

The contribution σ_s/R of disdrometer statistical error to AAD, as given by Eq. (16) (for a single DSD measurement) is depicted in Fig. 13 for $R(Z_H)$, $R(K_{DP})$ and $R(Z_H, Z_{DR})$. The variations of σ_s/R for $R_Q(Z_H, Z_V, K_{DP})$ is lower than that of $R(K_{DP})$. The response of the algorithms to statistical fluctuation is similar to their basic ability to track variations in the DSD. It is evident from Fig. 13 that at rain rates less than 20 mm h^{-1}, the AAD of $R(Z_H, Z_{DR})$ has larger σ_s/R than the AAD of other algorithms. This is due to the fact that the additional parameter Z_{DR} introduces its own statistical uncertainties which more than offset the ability

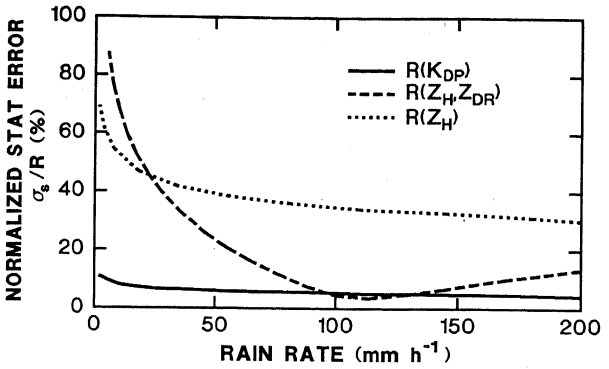

FIG. 13. Contributions σ_s/R to AAD of $R(Z_H)$, $R(Z_H, Z_{DR})$ and $R(K_{DP})$ as a function of rain rate for a single realization of the drop size distribution. $M-P$ relationship is used for $R(Z_H)$. The diameter and the sampling time of the disdrometer are 2 in and 25 s.

of Z_H and Z_{DR} to track DSD variations. This aspect also explains the performance of $R(Z_H, Z_{DR})$ for 4 June 1986 which has many more distributions with low rain rates (Fig. 4b) than that on 14 May 1986 (Fig. 4a). Also seen from Table 2 is that on 16 May 1986, which has the lowest number of distributions and also the lowest average rain rate, the difference between performance of $R(Z_H)$ and $R(Z_H, Z_{DR})$ is marginal. The AAD of $R(Z_H, Z_{DR})$ for this day includes larger contributions due to statistical measurement error than that included in the AAD of $R(Z_H)$.

The average rain rate and the number of DSDs considered for each day and the combined dataset are given in Table 1. From these and from Fig. 13 the σ_s/R for the results presented in Tables 2 and 3 are obtained. These are given in Table 4. σ_s/R in Table 4 would differ marginally if the rain rates for individual distributions are used instead of the average rain rate. From Table 4 it is apparent that for the combined dataset of 662 distributions, the statistical disdrometer measurement error contributes little to the AAD computed us ing $R(K_{DP})$. Hence we contend that the results of Tables 2 and 3 reflect its true DSD variability. However, in the case of $R(Z_H)$ and $R(Z_H, Z_{DR})$, the results in Tables 2 and 3 for the combined dataset includes σ_s/R of approximately 2% in addition to the DSD variability. Hence we contend that our comparisons are not unduly affected by the statistical measurement errors when the combined dataset is considered. This is further substantiated by the AAD of the combined dataset that is not significantly different from the dataset of day 134, which has 308 drop size distributions.

The variability due to DSD and the measurement error are statistically independent. Hence, from the knowledge of the statistical errors in polarimetric radar estimates and AAD due to DSD variation (Tables 2 and 3), it is possible to infer the variances in radar rainfall estimation. Using the formulation discussed in this section, it is also possible to estimate the expected scatter in the comparison of surface and radar measurements.

7. Summary and conclusions

Employing drop-size distributions obtained with a disdrometer, we have simulated rain rates derived from various polarimetric radar algorithms. These distributions gave rain rates that agreed very well with those obtained from a nearby rain gauge (Fig. 4). Simulated rain rates were derived based on $R(Z_H)$, $R_{ZDR}(Z_H, Z_{DR})$, $R(K_{DP})$ algorithms, and a new algorithm $R_Q(Z_H, Z_V, K_{DP})$. Comparisons of these radar algorithms were made under the same idealized conditions.

Using disdrometer measurements, we have demonstrated that serious biases dependent on the assumed maximum drop diameter, D_{max}, may exist in the $R_{ZDR}(Z_H, Z_{DR})$ method. Two maximum drop sizes in the polarimetric radar algorithms were tested; namely, $D_{max} = 7$ mm and $D_{max} = 5$ mm. Consistent offsets were found in simulated rain rates with respect to the disdrometer-derived rain rates for $D_{max} = 7$ mm (Fig. 8a). The smaller, more realistic D_{max} reduced this offset markedly (Fig. 8b) and produced better accuracies (AAD of 10.3%) in the R_{ZDR} method. This change in D_{max} caused a slight but insignificant revision in an empirical $R(K_{DP})$ relationship.

We stress that statistical errors and drop size distribution variations affect both radar-derived measurements and disdrometer-simulated rain measurements. Drop size distribution variations have the same effects on a given algorithm, but statistical variations are instrument dependent. These two errors cannot be easily separated from observations. The main thrust of simulations with disdrometer data is to reveal the sensitivities of algorithms to DSD variations. Therefore we have examined the statistics of instrumental errors in order to gauge their contribution to the total variability. We show that in the case of $R(Z_H, Z_{DR})$ at moderate rainfall rates ($\approx$20 mm h^{-1}) statistical errors of radar-derived and simulated measurements are comparable. This is in spite of the fact that variances of Z_H and Z_{DR} are larger in disdrometer simulations; these two variables are correlated and help reduce the total variance.

Rms errors in simulated rain rates for disdrometer derived $R(Z_H)$ and $R_{ZDR}(Z_H, Z_{DR})$ were 34% and 14% (Tables 2 and 3) in agreement with similar simulations by other investigators. The rms error in rain rate for $R(K_{DP})$ was found to be 10.4% (Table 3). A new relationship $R_Q(Z_H, Z_V, K_{DP})$ showed even a smaller error of 8% (Table 3). Because statistical errors of our

TABLE 4. The contribution of the statistical measurement errors, σ_s/R, to the AAD. The disdrometer diameter is 2 in and the sampling time is 25 s.

Day	$R(Z_H)$ σ_s/R (%)	$R(Z_H, Z_{DR})$ σ_s/R (%)	$R(K_{DP})$ σ_s/R (%)
134	2.52	2.35	0.39
136	4.55	6.14	0.70
155	3.42	4.26	0.53
Combined	1.83	2.0	0.28

disdrometer are such that the resulting rms errors in $R(K_{DP})$ is negligible, we conclude that the 10.4% error is caused by the DSD variability. It should not be construed that the R_Q algorithm would perform best in actual radar measurements. That is, because our simulations of R_Q was based on disdrometer data and does take into account such effects as statistical correlations among variables measured by the radar, calibration uncertainties, and statistical uncertainties associated with radar signals. Only single parameter measurements such as $R(Z)$ and $R(K_{DP})$ are unaffected by correlation effects. It turns out that the correlation effects on the variance of R_Q are small, and that it is mainly proportional to the variance of K_{DP}. If only DSD variations and statistical errors were significant, we predict that depending on rain rate, there is an optimum region for each algorithm. At less than 20 mm h^{-1} $R(Z_H)$ is expected to be optimum, between 20 and 40 mm h^{-1} $R(Z_H, Z_{DR})$ is optimum, and above 40 mm h^{-1} $R(K_{DP})$ is superior.

As a by-product, our study demonstrates that a disdrometer might be used instead of a rain gauge to determine needed adjustments, particularly in single-parameter radar algorithms. Where fixed polarization radars are measuring rain rates, a possible technique is to establish the least-squares-fit $R - Z$, using disdrometer measurements and applying this to the radar measured Z value to extract R. A separate $R - Z$ relationship may be realized for each rain type.

Acknowledgments. The authors are grateful to B. Musiani for reducing the original disdrometer data, to Drs. Sachidananda and Doviak for their continuing interest and useful suggestions, and to Mr. Bill Bumgarner for computational support. Ms. Carole Holder typed the manuscript and Ms. Joan Kimpel prepared the artwork. This work was partially supported by the Joint Systems Program Office of NEXRAD.

REFERENCES

Atlas, D., and C. W. Ulbrich, 1977: Path- and area-integrated rainfall measurement by microwave attenuation in the 1–3 cm band. *J. Appl. Meteor.*, **16,** 1322–1331.

Aydin, K., T. A. Seliga and V. Balaji, 1986: Remote sensing of hail with a dual linear polarization radar. *J. Clim. Appl. Meteor.*, **25,** 1475–1484.

Battan, L. J., 1973: *Radar Observation of the Atmosphere.* University of Chicago Press, 324 pp.

Chandrasekar, V., and V. N. Bringi, 1986: Problems in intercomparing radar measurements of rainfall with raindrop sampling devices. Preprints, *23rd Conference on Radar Meteorology,* Snowmass, Colorado, 112–115.

——, and ——, 1988: Error structure of multiparameter radar and surface measurements of rainfall. Part I: Differential reflectivity. *J. Atmos. Oceanic. Tech.*, **5,** 783–795.

Doviak, R. J., and D. S. Zrnić, 1984: *Doppler Radar and Weather Observations.* Academic Press, Inc., 458 pp.

Gertzman, H. S., and D. Atlas, 1977: Sampling errors in the measurement of rain and hail parameters. *J. Geophys. Res.*, **31,** 4955–5966.

Goldhirsh, J., 1979: A review of the application of nonattenuating frequency radars for estimating rain attenuation and space-diversity performance. *IEEE Trans. Geosci. Remote Sens.*, **GE-17**(4), 218–239.

——, 1980: Space-diversity performance comparison of radar derived slant path rain attenuations with the COMSTAR beacon fates at 28.56 GHz for summer and winter periods. *IEEE Trans. Antennas Propag.*, **AP-28**(4), 577–580.

——, and B. Musiani, 1986: Rain cell size statistics derived from radar observations at Wallops Island, Virginia. *IEEE Trans. Geosci. Remote Sens.*, **GE-24**(6), 947–957.

——, J. Rowland and B. Musiani, 1987: Rain measurement results derived from a two-polarization frequency—diversity S-band radar at Wallops Island, Virginia. *IEEE Trans. Geosci. Remote Sens.*, **GE-25**(6), 654–660.

Gunn, R., and G. D. Kinzer, 1949: The terminal velocity of fall for water droplets in stagnant air. *J. Meteor.*, **6,** 243–248.

Jameson, A. R., 1985: Microphysical interpretation of multiparameter radar measurements in rain. Part III: Interpretation and measurement of differential phase shift between orthogonal linear polarizations. *J. Atmos. Sci.*, **42,** 607–614.

——, 1986: The dependence of microwave attenuation and propagation phase shift on raindrop sizes and shapes. Preprints, *23rd Conference on Radar Meteorology,* Snowmass, Colorado, 96–99.

Joss, J., and A. Waldvogel, 1969: Raindrop size distribution and sampling size errors. *J. Atmos. Sci.*, **26,** 566–569.

——, and E. G. Gori, 1978: Shapes of raindrop size distributions. *J. Appl. Meteorol.*, **17,** 1054–1061.

Leitao, M. J., and P. A. Watson, 1984: Application of dual-linearly polarized radar data to prediction of microwave path attenuation at 10–30 GHz. *Radio Sci.*, **19,** 209–221.

McCormick, G. C., and A. Henry, 1975: Principles for the radar determination of the polarization properties of precipitation. *Radio Sci.*, **10,** 421–434.

Mueller, G. A., 1984: Calculation procedure for differential propagation phase shift. Preprints, *22nd Conference on Radar Meteorology,* Zurich, Switzerland, 397–399.

Oguchi, T., 1983: Electromagnetic propagation and scattering in rain and other hydrometeors. *Proc. IEEE,* **71,** 1029–1078.

Pruppacher, H. R., and K. V. Beard, 1970: A wind tunnel investigation of internal circulation and shape of water drops falling at terminal velocity in air. *Quart. J. Roy. Meteor. Soc.*, **96,** 247–256.

Ray, P. S., 1972: Broadband complex refractive indices of ice and water. *Appl. Opt.*, **11,** 1836–1844.

Rowland, J. R., 1976: Comparison of two different raindrop disdrometers. *17th Conference on Radar Meteorology,* Seattle, Washington, 398–405.

Sachidananda, M., and D. S. Zrnić, 1986: Differential propagation phase shift and rainfall rate estimation. *Radio Sci.*, **21,** 235–247.

——, and ——, 1987: Rain rate estimates from differential polarization measurements. *J. Atmos. Oceanic Tech.*, **4**(3), 588–598.

Seliga, T. A., and V. N. Bringi, 1976: Potential use of radar reflectivity measurements at orthogonal polarizations for measuring precipitation. *J. Appl. Meteor.*, **15,** 69–76.

——, and ——, 1978: Differential reflectivity and differential phase shift: Applications in radar meteorology. *Radio Sci.*, **13**(2), 271–275.

——, K. Aydin and H. Direskeneli, 1986: Disdrometer measurements during an intense rainfall event in central Illinois: Implications for differential reflectivity and radar observables. *J. Clim. Appl. Meteor.*, **25,** 835–846.

Ulbrich, C. W., 1985: The effect of dropsize distribution truncation on rainfall integral parameters and empirical relations. *J. Clin. Appl. Meteor.*, **24,** 580–590.

——, and D. Atlas, 1984: Assessment of the contribution of differential polarization to improved rainfall measurements. *Radio Sci.*, **19,** 49–57.

Wong, R. K. W., and N. Chidambaram, 1985: Gamma size distribution and stochastic sampling errors. *J. Clim. Appl. Meteor.*, **24,** 568–579.